



ISSN: 1813-162X (Print); 2312-7589 (Online)

Tikrit Journal of Engineering Sciences

available online at: <http://www.tj-es.com>
TJES
Tikrit Journal of
Engineering Sciences

Assessing the Eco-Environmental Quality of Kirkuk City and Taza District Based on Pressure-State-Response Framework for Two Seasons Using Remote Sensing and GIS

Sundus Mohammed Azeez *, **Muntadher Aidi Shareef** , **Fawzi Mardan Omer**

Surveying, Engineering Technical College- Kirkuk, Northern Technical University, Mosul, Iraq.

Keywords:

Eco-environmental; Ecological index; Pressure indicator; PSR framework; Response indicator; Sentinel-2; State indicator.

Highlights:

- PSR framework with 12 RS indicators assesses Kirkuk/Taza eco-environmental quality.
- Winter shows healthier ecology than summer due to reduced human activity.
- Sentinel-2 & GIS reveal direct link between human pressure and ecological degradation.

ARTICLE INFO**Article history:**

Received	24 Mar. 2024
Received in revised form	25 June 2024
Accepted	25 July 2024
Final Proofreading	10 June 2025
Available online	18 Aug. 2025

© THIS IS AN OPEN ACCESS ARTICLE UNDER THE CC BY LICENSE. <http://creativecommons.org/licenses/by/4.0/>



Citation: Azeez SM, Shareef MA, Omer FM. Assessing the Eco-Environmental Quality of Kirkuk City and Taza District Based on Pressure-State-Response Framework for Two Seasons Using Remote Sensing and GIS. *Tikrit Journal of Engineering Sciences* 2025; 32(3): 2105. <http://doi.org/10.25130/tjes.32.3.13>

***Corresponding author:****Sundus Mohammed Azeez**

Surveying, Engineering Technical College- Kirkuk, Northern Technical University, Mosul, Iraq.

Abstract: Evaluating a region's Ecological Environment Quality (EEQ) is an essential factor in determining its rate of urbanization and sustainable development. This study aims to determine the Ecological Index (EI) and evaluate it using the widely used pressure-state-response (PSR) framework based on a set of statistical and remote sensing indices in Kirkuk City and Taza District. Sentinel-2 satellite images were used to obtain 12 indicators created from remote sensing for assessing eco-environmental quality. These indicators provide a foundation for sustainable development decision-making, offering new and cutting-edge technological support for long-term, thorough mapping and monitoring. The study compares the Ecological Index of Kirkuk City and Taza District during the winter and summer seasons of 2023. The findings revealed that the ecological condition was healthier in winter than in summer, primarily due to the atmospheric conditions and reduced social and economic activities. Additionally, the findings presented the main relationship between environmental health and human activities under different weather conditions.

تقييم جودة النظام البيئي في محافظة كركوك ومقاطعة تازة بالاعتماد على طريقة Pressure-State-Response Framework لفصلين باستخدام التحسس الثنائي ونظم المعلومات الجغرافية

سندس محمد عزيز، منتظر عدي شريف، فوزي مردان عمر
قسم تقنيات هندسة المساحة/ الكلية التقنية الهندسية-كركوك / الجامعة التقنية الشمالية/ الموصل – العراق.

الخلاصة

تقييم النظام البيئي لمنطقة ما، هو عامل مهم في تحديد معدل التطور العمراني والتنمية المستدامة. تهدف هذه الدراسة لإيجاد المؤشر البيئي (EI) وتقييمه بواسطة الطريقة الشائعة pressure-state-response (PSR) framework بالاعتماد على مجموعة من المؤشرات الإحصائية والخاصة بالتحسس الثنائي في مدينة كركوك ومقاطعة تازة. تم استخدام الصور الفضائية sentinel-2 للحصول على ١٢ من المؤشرات التي تم صنعها من التحسس الثنائي لتقييم جودة النظام البيئي. هذه المؤشرات توفر أساساً لصناعة القرار في التنمية المستدامة كتقنية حديثة تدعم التغير الذي يحدث على المدى البعيد من خلال انشاء الخرائط وعرضها تقوم هذه الدراسة بمقارنة المؤشر البيئي لفصل الشتاء وفصل الصيف لسنة ٢٠٢٣ في محافظة كركوك ومقاطعة تازة. يشير البحث الى ان الحالة البيئية تبدو أكثر صحة في فصل الشتاء منه في فصل الصيف وذلك تبعاً للظروف الجوية والنشاط الاجتماعي والاقتصادي للإنسان بالإضافة الى ان البحث يظهر العلاقة الرئيسية بين الصحة البيئية والنشاط البشري في مختلف الظروف الجوية.

الكلمات الدالة: بيئة اقتصادية؛ مؤشر بيئي؛ مؤشر الضغط؛ إطار عمل المسؤولية الاجتماعية للشركات؛ مؤشر الاستجابة؛ سنتيل-٢؛ مؤشر الحالة.

1. INTRODUCTION

Eco-environmental assessment has become increasingly important over the last five decades, particularly in decision-making for environmental management and quality assurance. The Ecological Index is a key component of these management acts and one of the most effective policies to limit all types of pollution and their negative impacts [1]. The cornerstone and basis of a region's sustainable socioeconomic development is its eco-environmental quality. Evaluation of the eco-environmental quality can indicate how well social production and the living environment are coordinated, as well as a region's capacity for sustained socioeconomic development [2]. Since the natural environment supplies resources, such as water, land, biological resources, and climate, among others, it is crucial for human life and progress [3]. As the natural environment has undergone significant changes in emerging nations over recent decades, it is crucial to monitor and understand the state of the ecosystem. Due to its ability to provide extensive and dynamic compliance, remote sensing technology has proven invaluable in ecological monitoring [4]. On the other hand, the pressure-state-response (PSR) model emphasizes the importance of humans as part of the ecosystem and their impact on the status of environmental resources and social pressures, which are two examples of the stresses that human activity imposes on the ecosystem's health [5]. The vitality, structure, and resilience of an ecosystem are examples of state indicators that show the current state of ecosystem health. The response indicators demonstrate how an ecosystem responds to changes in its overall health, including those induced by both human activities and the ecosystem's natural processes [6]. These factors can also impact plant growth by influencing changes in soil temperature, land use/cover, greenness, heat, soil texture, and dryness. As a

result, since all ecological indicators are either directly or indirectly relevant, any disruption or change in one ultimately affects or disrupts the entire ecosystem [7]. Land-use changes and eco-environmental quality index changes were connected. For example, the rapid growth of residential areas increases the amount of land with poor environmental quality. However, a complicated combination of anthropogenic factors, such as population growth and economic development, and natural factors, such as temperature and precipitation, drives changes in eco-environmental quality and ecological parameters [8]. Maps of land use and cover are crucial for advancing our understanding of environmental modeling and water management [9]. The Organization for Economic Cooperation and Development (OECD) first suggested the Pressure-State-Response (PSR) framework for determining environmental policy. It can combine a collection of statistics and remote sensing data into a single index using a weighting technique, such as the Analytical Hierarchy Process (AHP) [10]. Although they overlap and are frequently used interchangeably, terms like "livability," "living quality," "living environment," "quality of place," "residential perception and satisfaction," "evaluation of the residential and living environment," "quality of life," and "sustainability" are also occasionally contrasted [11]. The numerous theories are rooted in the history of study and policymaking related to health, safety, well-being, residential satisfaction, and the physical environment of cities [12]. This study aims to evaluate the eco-environmental system in Kirkuk City and Taza, as this issue has become a leading subject in research worldwide, with a direct relation to people's health and quality of life. Therefore, limiting the pollutants and preparing the path for taking serious measures are much easier and faster. This paper examines the impact of

human activities and climate change on the ecological system by comparing five ecological responses across two seasons, i.e., winter and summer, within a single year.

2. MATERIALS AND DATA ACQUISITION

2.1. Study Area

The City of Kirkuk is located in the northwest of Iraq. The city is bordered by the Zagros Mountains to the north, the Hamrin Mountains to the south, the lower Zab Mountains to the west, and Al-Sulaymaniyah City to the east. Geographically, Kirkuk City is situated between latitude $35^{\circ} 13'$ and $36^{\circ} 29' N$ and longitude $44^{\circ} 00'$ to $44^{\circ} 50' E$. The city's total area is approximately $9,679 \text{ km}^2$ [13]. The distance from Baghdad, the capital of Iraq, is approximately 250 kilometers (Fig. 1). The study area experiences a semiarid and

Mediterranean climate characterized by hot and dry summers as well as cold winters. The majority of the precipitation occurs between December and March, while the summer months receive little to no rainfall [9]. Temperature plays a significant role in the climate, with peak temperatures reaching approximately $48^{\circ} C$ during the summer and dropping to a low of $-1^{\circ} C$ in the winter. The city of Kirkuk is situated in the hilly northern part of the Kirkuk plain, approximately 340-360 meters above sea level. The Kirkuk structure, also known as the Baba Dome, and the Hamrin structure mark the northern and eastern boundaries of the plain, while the Hamrin structure and the lower Zap River outline the western and northern margins [13].

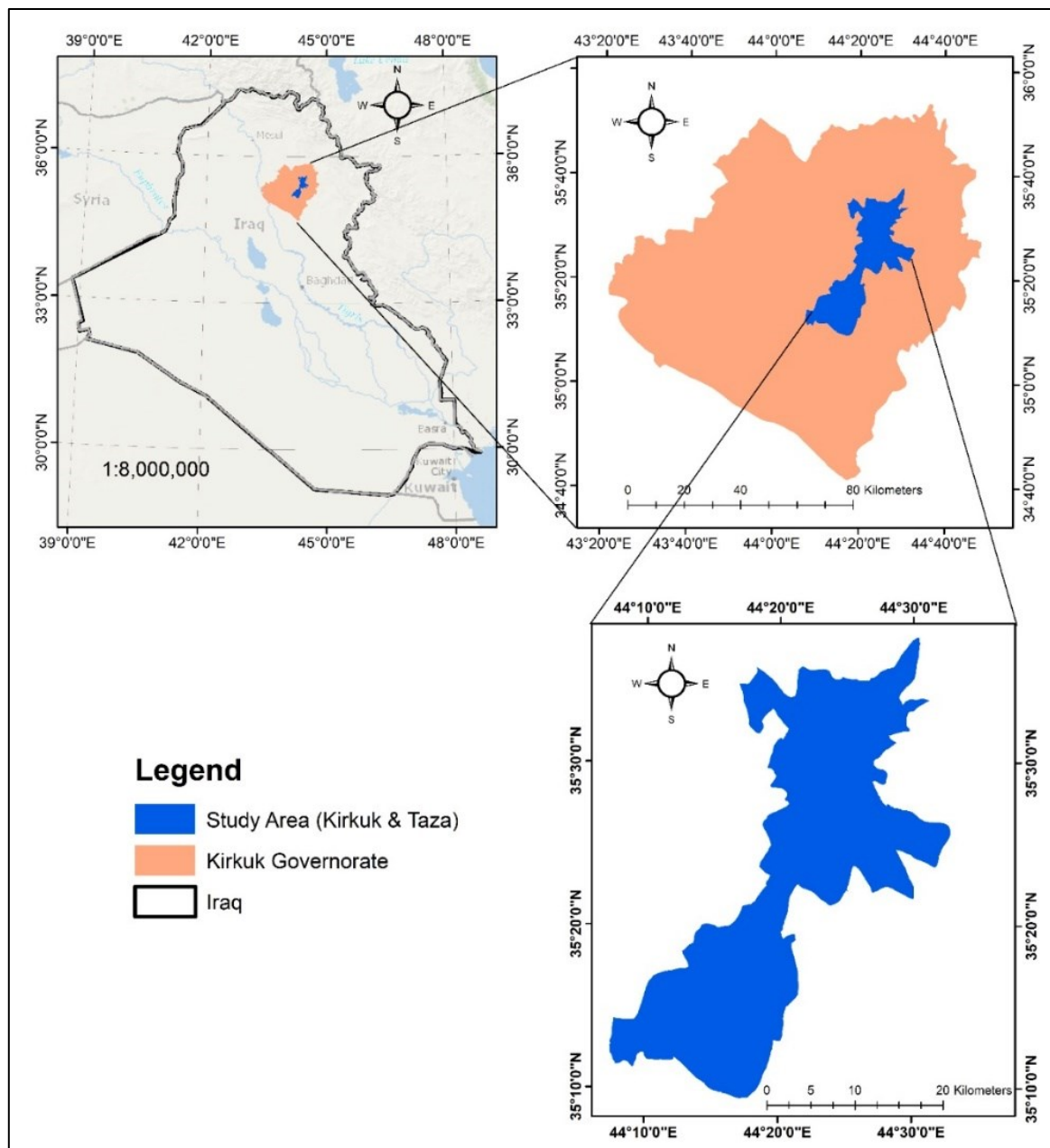


Fig. 1 The Study Area of Kirkuk City and Taza District.

2.2.Data and Pre-Processing

2.2.1.Data Used

This study used Sentinel-2 data, including (level-2A) images. The satellite features an optoelectronic multispectral sensor with 13 spectral channels, enabling surveying in the visible, near-infrared (VNIR), and shortwave

infrared (SWIR) spectral zones at Sentinel-2 resolution of 10 to 60 m (image details are provided in Table 1). All images were downloaded for free from the Copernicus website (a part of the European Union's space program) with a cloud coverage of less than 2% for summer and winter seasons.

Table 1 Band Details of Sentinel Two Satellite Image.

Bands (wavelength region)	Central wavelength (nm)	Resolution (m)
Band-1 (coastal aerosol)	443	60
Band-2 (blue)	490	10
Band-3 (green)	560	10
Band-4 (red)	665	10
Band-5 (vegetation red edge)	705	20
Band-6 (vegetation red edge)	740	20
Band-7 (vegetation red edge)	783	20
Band-8 (NIR)	842	10
Band-8A (vegetation red edge)	865	20
Band-9 (water vapour)	945	60
Band-10 (SWIR-Cirrus)	1375	60
Band-11 (SWIR)	1610	20
Band-12 (SWIR)	2190	20

2.2.2.Data Pre-Processing

All images were resampled using bilinear interpolation, which enables seamless switching between pixels throughout the resizing or scaling process. By utilizing the values of neighboring pixels, the process of approaching new pixel values helps minimize the presence of pixelation and aliasing objects, thereby enhancing the quality and visual appeal of images. Geometric and atmospheric corrections were not applied because these types of images are atmospherically corrected surface reflectance in cartographic geometry. The ortho-images, or granules, are 110×110 km² and are projected using the UTM/WGS84 coordinate system. Moreover, the Earth is divided into a 100 km step and a predetermined set of tiles defined in the UTM/WGS84 projection. Nonetheless, every tile features a surface area of 110×110 km², enabling substantial overlap with adjacent tiles. The two images of the winter and summer seasons were found to be overlapped geospatially in registration, which means that all pixels represent the exact location in both images.

3.METHODS

The method adopted in this study to obtain the ecological index utilizes the pressure-state-response (PSR) framework, which utilizes nine indicators to determine the Pressure Indicator and three to assess the State Indicator. All indicators were obtained using SNAP 9.0.0 software and were output using ArcGIS 10.7 software. The equations were applied using GIS 10.7 software. On the other hand, the Pressure Indicators were included in the Digital

Elevation Model (DEM), Global Environmental Monitoring Index (GEMI), Land Use/Cover (LULC), Normalized Difference Moisture Index (NDMI), Normalized Difference Water Index (NDWI), Soil Adjusted Vegetation Index (SAVI), Road network and Railway network, Land Surface Temperature (LST). The state indicators were included from Fractional Vegetation Cover (FVC), Normalized Leaf Area Index (LAI), and Normalized Difference Vegetation Index (NDVI).

To ensure that each indicator has a comparable weight and significance in the outcome, all indicators were rescaled and normalized from 0 to 1. The overall methodology is explained in Fig. 2.

3.1.1.Indicators used

3.1.1.Global Environmental Monitoring Index (GEMI)

A nonlinear vegetation index for worldwide environmental monitoring, GEMI, is created from satellite data. Although it is comparable, the Normalized Difference Vegetation Index (NDVI) is less susceptible to atmospheric impacts. Because GEMI is impacted by bare soil, it is not recommended for use in locations with moderately to heavily vegetated areas. The GEMI value is a number between 0 and 1, where 0 represents no vegetation cover, and 1 represents total vegetation cover over the ground [14]. The influence of emissions reflected into the atmosphere, mainly from vegetated areas, can be extracted and measured using GEMI [15]. Figure 3 shows the GEMI, where (A) represents the winter season, and (B) represents the summer season.

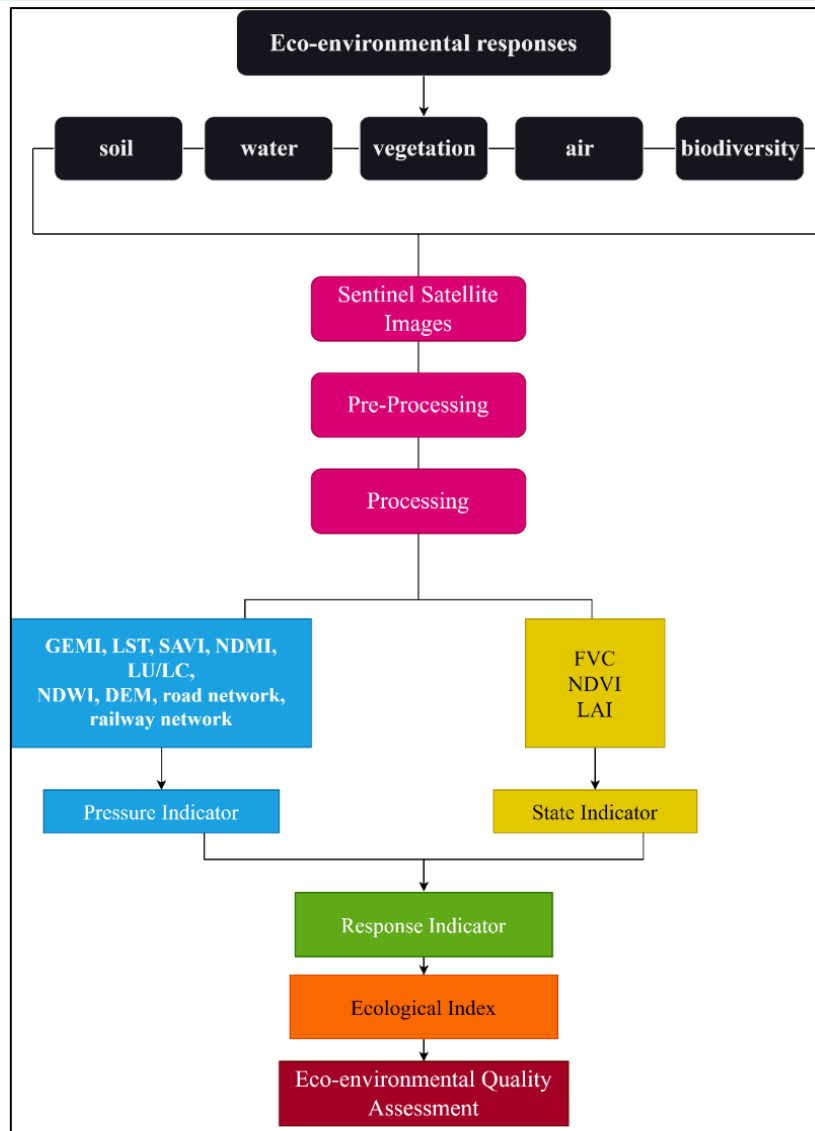


Fig. 2 The Overall Methodology.

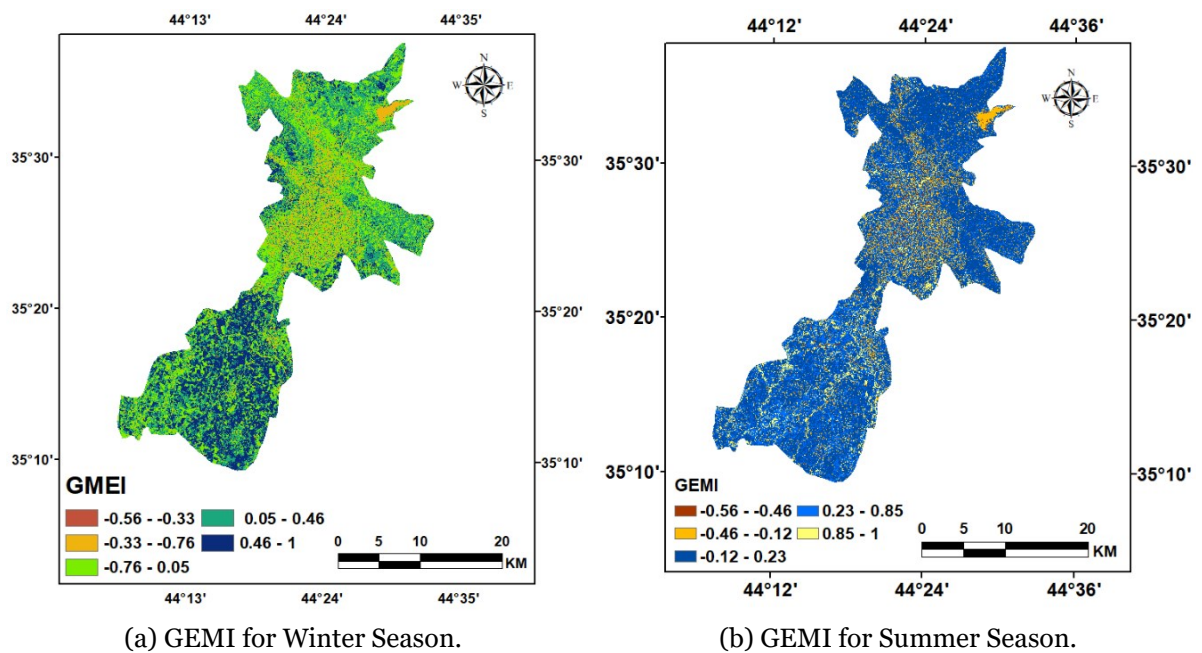


Fig. 3 GEMI for Winter and Summer Seasons.

3.1.2. Fractional Vegetation Cover (FVC)

FVC is a crucial metric in the study of soil erosion, climate change, and ecosystem balance. FVC is frequently employed in the assessment and tracking of vegetation degradation and desertification. FVC is an estimated proportion of the entire research area covered by vegetation, including leaves, stems, and roots. Also, FVC is a measurement of the vegetation's spatial distribution on the ground surface. The range of FVC values is 0 to 1, where 0 denotes no vegetation cover, and 1 denotes total plant cover over the ground surface [16]. Although minor breaks in the vegetation cover and sun flecks at the surface are permissible, the portion of the vegetation canopy known as the FVC has no patches of bare soil between plants [17]. Figure 4 shows the obtained FVC, where (A) represents the winter season, and (B) represents the summer season.

3.1.3. Leaf Area Index (LAI)

Plant canopies are characterized by a dimensionless quantity called the Leaf Area Index (LAI). LAI's range varies depending on the type of canopy and the specific conditions. LAI values can generally be found between 0 (bare ground) and over 10 (thick conifer forests) [18]. The leaf area to per unit ground surface area ratio is known as the LAI and is a dimensionless variable. The processes of gas-vegetation exchange, such as photosynthesis, may be linked to this ratio [19]. Figure 5 shows the LAI, where (A) represents the winter season, and (B) represents the summer season.

3.1.4. Normalized Difference Moisture Index (NDMI)

NDMI is not standardized. The index is straightforward to understand, with values ranging from -1 to 1; higher values indicate healthier and denser vegetation [20]. The NDMI technique is utilized to get moisture content by utilizing near-infrared (NIR) and shortwave infrared (SWIR) spectra [21]. This indicator's two most popular uses are to track vegetation moisture content and drought stress. The dry matter content of leaves is highly correlated with the NDMI indices [22]. Figure 6 shows the NDMI, where (A) represents the winter season, and (B) represents the summer season.

3.1.5. Normalized Difference Vegetation Index (NDVI)

Using sensor data is a commonly used metric to measure the density and health of plants. It is computed using spectrometric data in the near-infrared and red wavelengths. The index is simple to comprehend, with values ranging from -1 to 1; higher values denote healthier and denser vegetation [20]. The index is simple to comprehend, with values ranging from -1 to 1 [20]. The index benefits from the circumstance in which features with low red light reflectance and very low NIR reflectance (such as water) are suppressed or even eliminated, while those with high NIR reflectance and lower red light reflectance (such as terrestrial vegetation) are enhanced [23]. Figure 7 shows the NDVI, where (A) represents the winter season, and (B) represents the summer season.

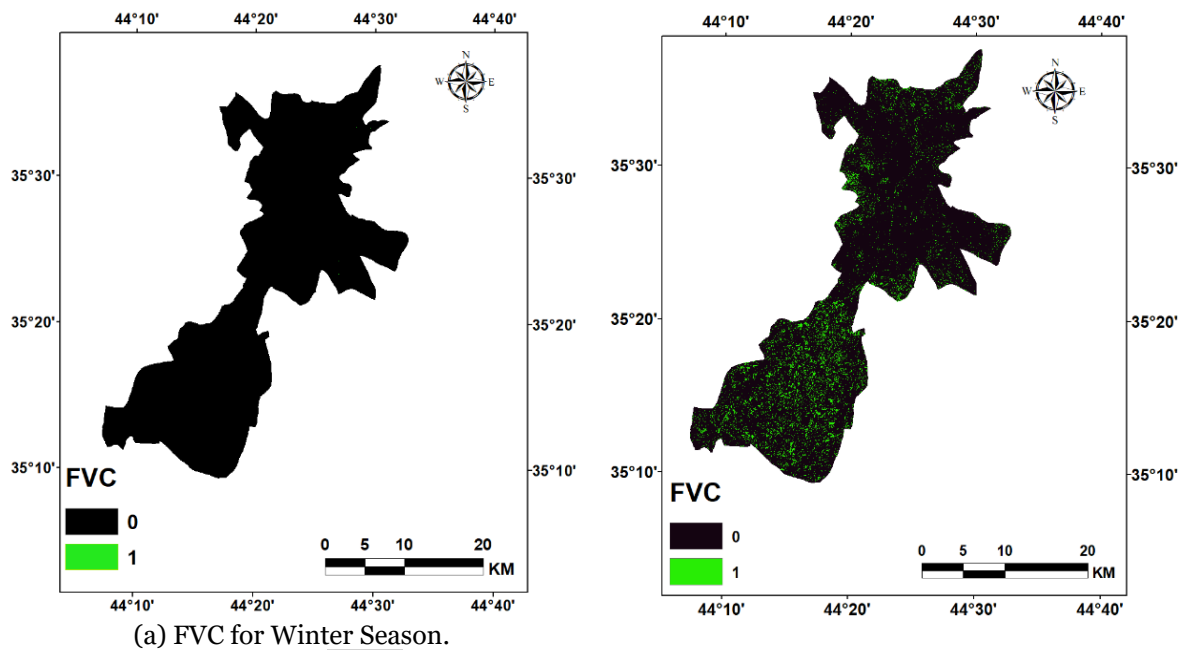


Fig. 4 FVC for Winter and Summer Seasons.

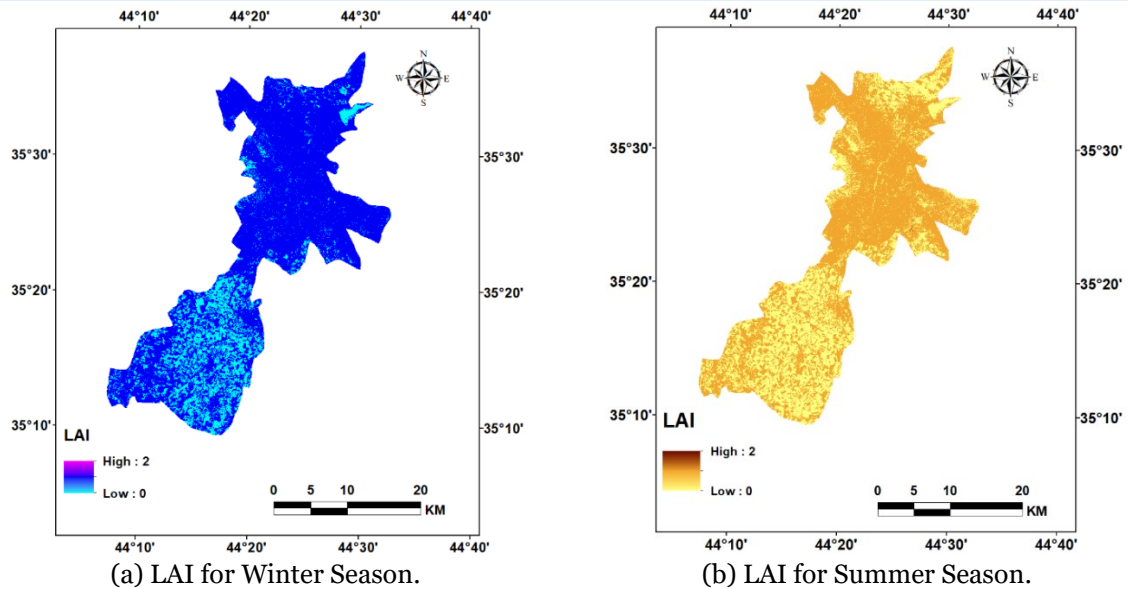


Fig. 5 LAI for Winter and Summer Seasons.

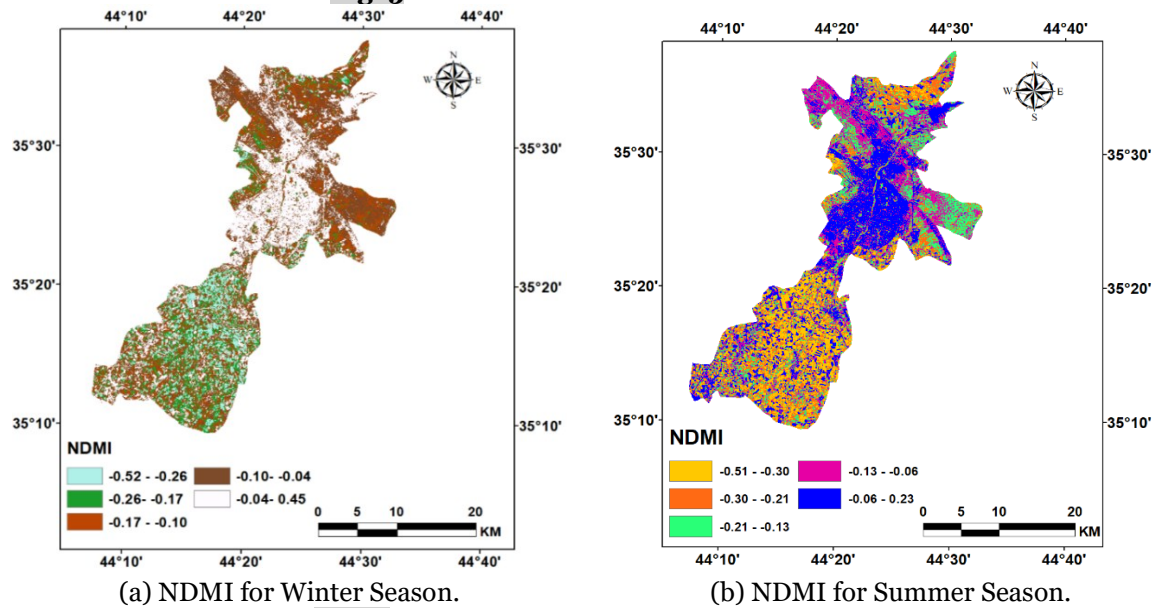


Fig. 6 NDMI for Winter and Summer Seasons.

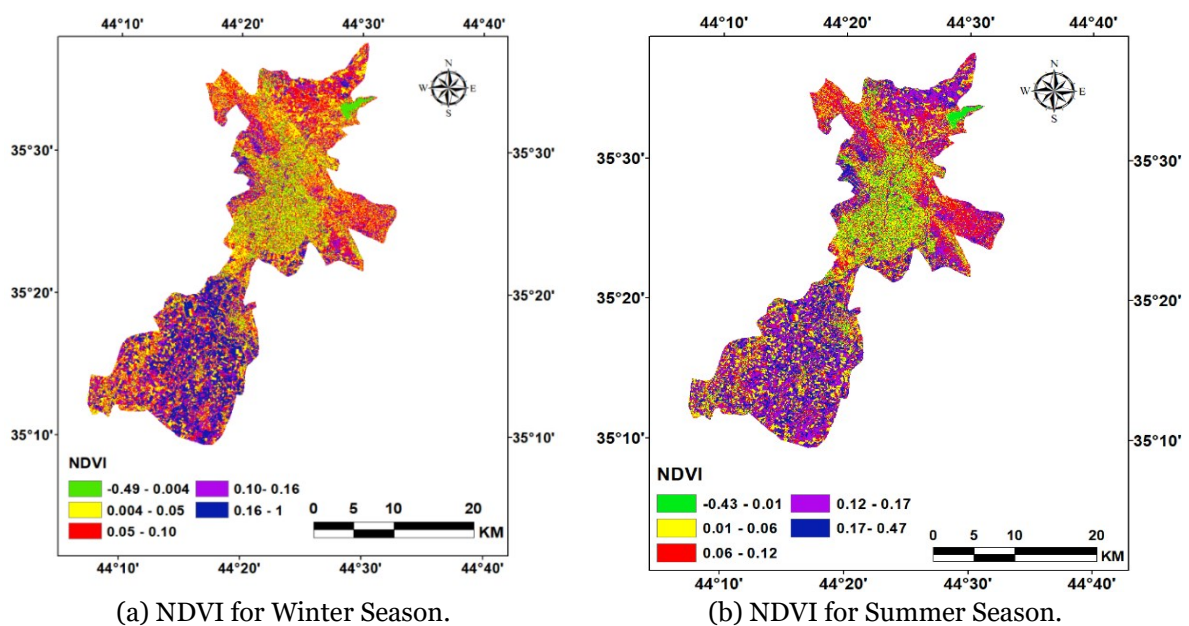


Fig. 7 NDVI for Winter and Summer Seasons.

3.1.6. Normalized Difference Water Index (NDWI)

NDWI is a commonly used metric that uses sensor data to quantify the density and health of vegetation. It is computed using spectrometric data in the near-infrared and red wavelengths. The index is simple to understand, with values ranging from -1 to 1. High values denote healthier and denser vegetation. Although spectrum-matching techniques are inappropriate for determining the liquid water content of vegetation from data obtained with these sensors, the NDWI can still be used to obtain information on the liquid water content of vegetation [24]. Figure 8 shows the NDWI, where (A) represents the winter season, and (B) represents the summer season.

3.1.7. Railway and Road Network

The analysis of human strain on the ecosystem can be done using a nation's road and rail networks, among other infrastructure and utility. More significant changes indicate a higher frequency of human activity. High population density is correlated with a higher density of roads, facilitating greater movement frequencies. Before utilization, it was transformed into a 10 m pixel raster format, facilitating seamless integration with reaming satellite data. Primary (national highway), secondary (state highway), residential, and local roads (including footpaths) are among the types of road data in the research area. [7]. The increase in traffic resulting from projects could be offset by additional highway funding [25]. The estimated railway and road networks are shown in Fig. 9, where (A) is the road network map, and (B) is the railway network map.

3.1.8. Land Use/Land Cover

Information regarding land use and cover is essential for numerous reasons, including those

related to planning, decision-making, the spread and primary needs of human populations, and health [26]. The evaluation of land use and vegetation cover, as well as their changes, is crucial for decision-makers in designing cities and developing future strategies to address urban growth. This issue is crucial due to the increasing size of buildings and the expansion of urban areas and populations [27]. Inventories, the ideas of land use, and land cover are usually combined. Terrestrial ecosystems, natural resources, and habitats are all characterized by land cover, a crucial component of climate models. Direct observation can be used to ascertain it. Ecosystem function and social, economic, and cultural utility are described by land use. It necessitates the interpretation of the socioeconomic activity occurring there [28]. The Support Vector Machine (SVM) classification method was used to obtain classes represented by urban areas, water bodies, barren areas, agricultural areas, and vegetation. The classification is shown in Fig. 10, where (A) represents the winter season, and (B) represents the summer season.

3.1.9. Soil-Adjusted Vegetation Index (SAVI)

Using a soil brightness adjustment factor, SAVI is a vegetation index designed to reduce the effects of soil brightness. It is frequently employed in dry areas with little vegetation cover. Higher values indicate denser and healthier vegetation. The SAVI values range from -1.0 to 1.0 [29]. The development of basic "global" models that can characterize dynamic soil-vegetation systems using remotely sensed data has significantly benefited from the SAVI [30]. Figure 11 shows the SAVI, where (A) represents the winter season, and (B) represents the summer season.

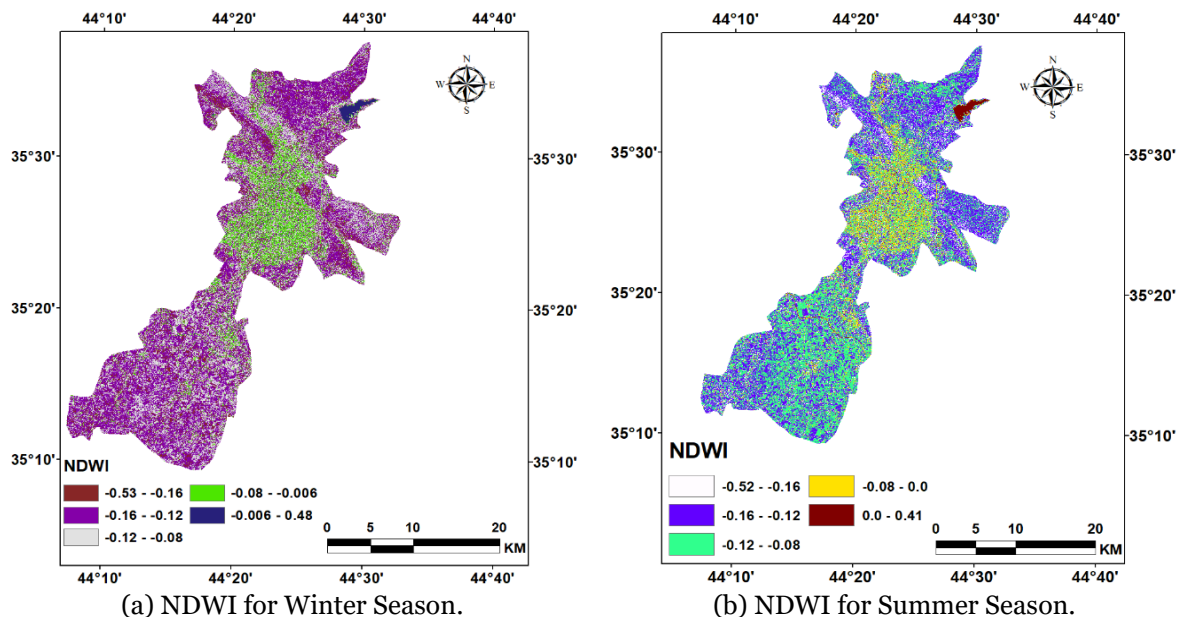
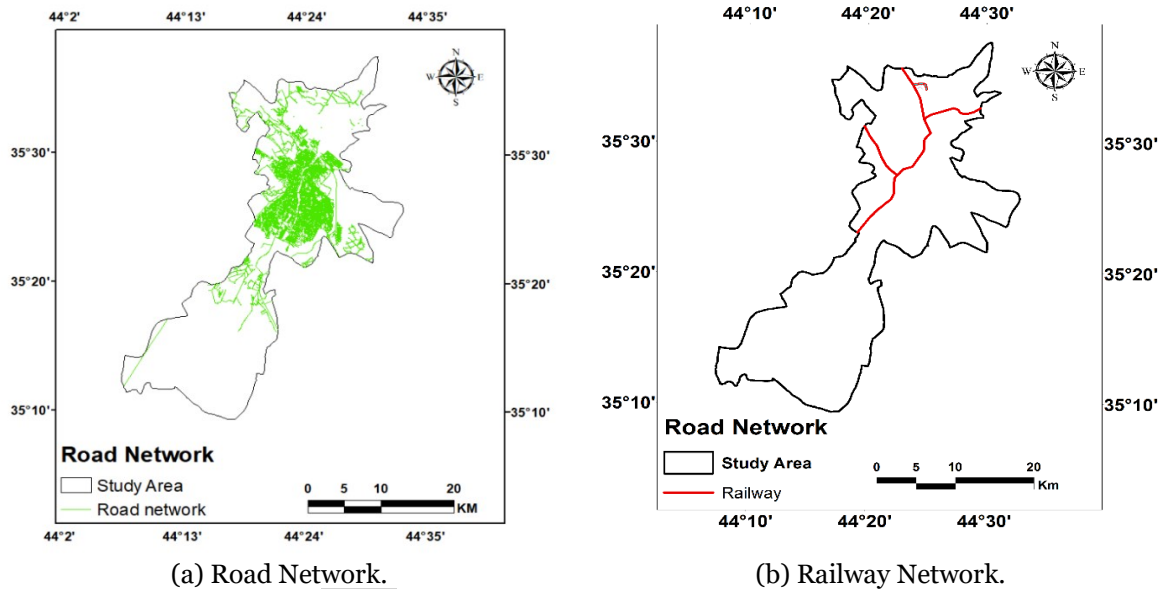
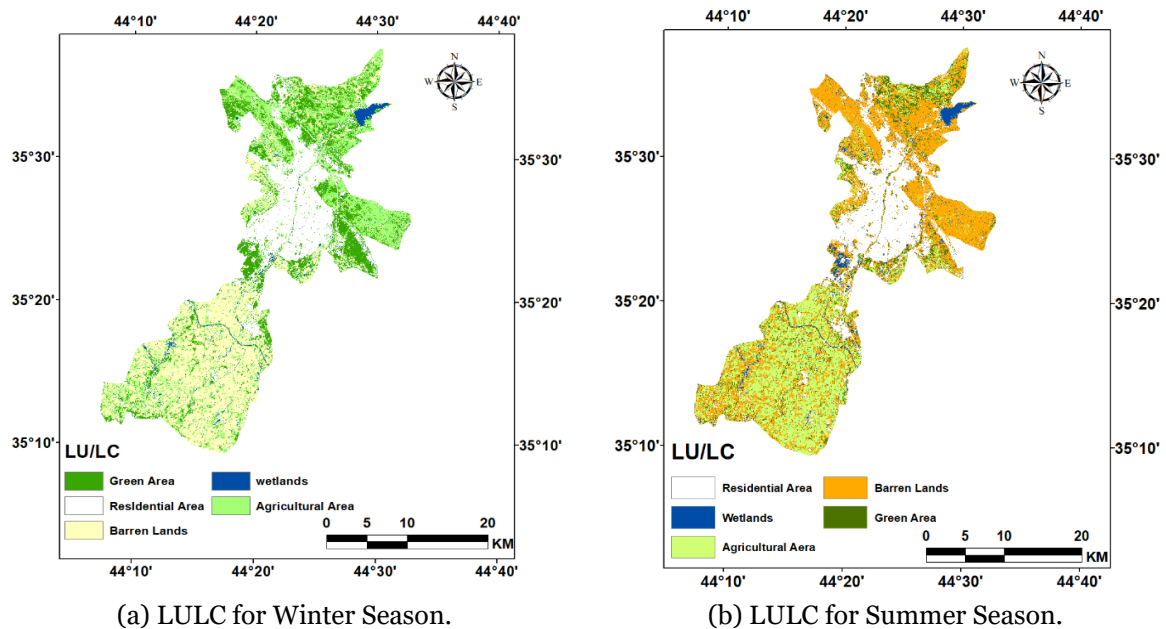
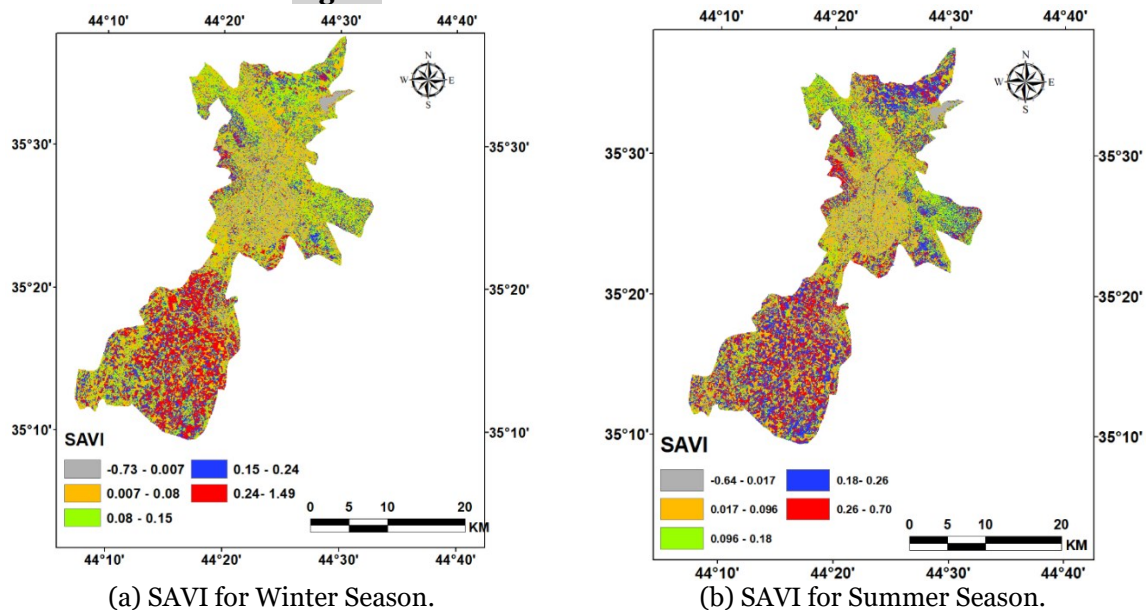


Fig. 8 NDWI for Winter and Summer Seasons.

**Fig. 9** Road Network and Railway Network.**Fig. 10** LULC for Winter and Summer Seasons.**Fig. 11** SAVI for Winter and Summer Seasons.

3.1.10. Digital Elevation Model (DEM)

One of the most significant spatial datasets in many geographical information systems (GIS) is a digital elevation model (DEM). To represent terrain, it is described as an ordered or unordered digital set of ground elevation (spot height) [31]. The majority of a catchment's water balance is influenced by topography, a significant land-surface feature. These elements include the production of surface and subsurface runoff, the flow pathways that water takes when it descends and traverses' hillslopes, and the rate of water movement. The topography (represented by the DEM of the area modeled) is used by all of the spatially explicit, fully distributed hydraulic and hydrological models to determine bathymetry. Several important details necessary for adequately distributed hydraulic and hydrological models are also derived using DEM [32]. The DEM used in this study is represented in Fig. 12.

3.1.11. Land Surface Temperature (LST)

The sparse and irregular distribution of weather observatories, the challenges

associated with conducting field surveys, and the complicated nature of interpolating station data present obstacles to the continuous monitoring of harsh settings. Therefore, remotely sensed land surface temperature (LST) is very interesting for a range of biological and environmental applications [33]. It is a crucial factor that significantly influences the radiative energy budget of the Earth's surface. The land surface temperature (LST) is an essential input for land-surface models that monitor dryness, estimate soil moisture, and calculate evapotranspiration, as it drives the turbulent heat exchanges and outgoing long-wave radiation at the interface between the land and the atmosphere [34]. One of the main indicators characterizing the surface environment is surface temperature, which is directly correlated with the development and distribution of vegetation and the evaporation cycle of surface water resources [35]. Figure 13 shows the obtained LST, where (A) represents the winter season, and (B) represents the summer season.

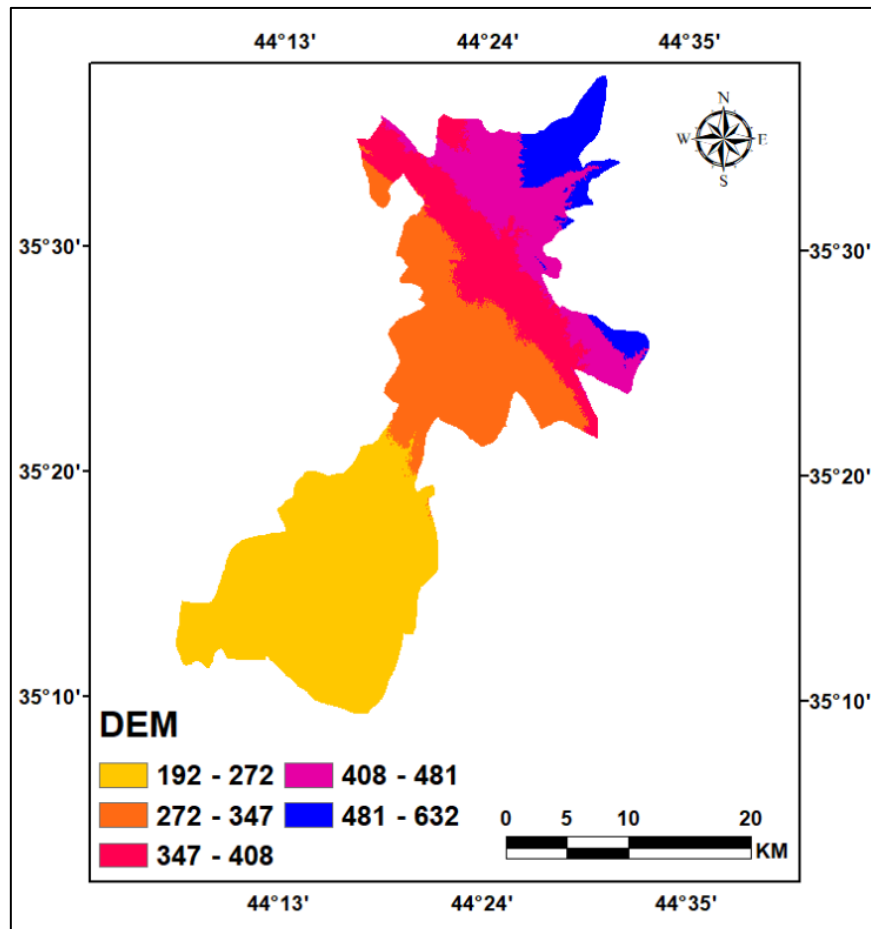


Fig. 12 Digital Elevation Model (in Meters) of Kirkuk City and Taza District.

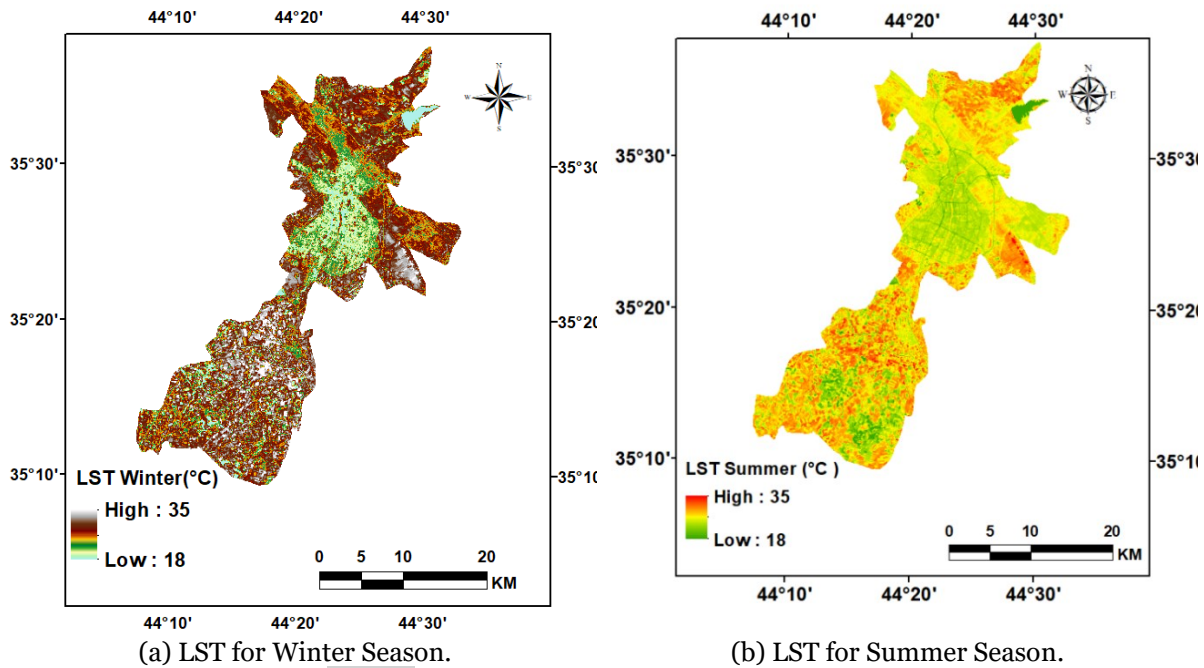


Fig. 13 LST for Winter and Summer Seasons.

3.2.PSR Framework

The Pressure-State-Response (PSR) framework alters environmental state (condition) factors in response to pressures on the environment resulting from human activity. It extends beyond the constraints of flat-dimensional indicator sets, providing more detailed information on the impact of human activities on ecosystems. The PSR method addresses the factors that contribute to a quantifiable state. It is broken down into three categories of indicators: Pressure Indicator (PI), State Indicator (SI), and Response Indicator (RI) [36]. The dynamic and systematic interactions between the economic, social, and ecological environments can be reflected in the three dimensions of the PSR framework [37].

3.2.1.Pressure Indicator (PI)

The stresses that human activity places on the health of ecosystems are described by pressure

$$PI = \frac{GEMI + SAVI + NDMI + LULC + Road + Rail + LI + NDWI + DEM}{9} \quad (1)$$

3.2.2.State Indicator (SI)

State indicators, which include an ecosystem's strength, organization, and resilience, show the current state of ecosystem health [38]. Healthy natural phenomena, such as NDVI, LAI, FVC, forests, mangroves, wetland wetlands, and waterbodies, are generally indicative of healthy ecosystems. These land cover classes indicate a healthy state of the ecosystem and are characterized by minimal to no human interaction, activity, or disturbance. All parameters were first standardized to a range of 0 to 1 and then given equal weight, according to Eq. (2), to generate the state indicator. Better

indicators (PIs), which include social and resource demands. [38]. The PI value from standardized data ranges from 0 to 1, giving each indicator in the research region equal weight, as shown in Eq. (1) [7]. The questions of "What has been done?" and "What should be done?" are addressed by the response indicators of human countermeasures for environmental problems. These indicators demonstrate that society works to address environmental issues and track the state of environmental policy implementation for environmentally sustainable development [38]. Depending on the concerns or progress that need to be addressed, the indicators of a PSR framework can be chosen accordingly. There would not be a standard set of indicators, and the choices might differ depending on the nation or the location. Data accessibility is still another crucial factor [39].

ecological conditions are indicated by higher SI values, and worse ecological conditions are indicated by lower values [7].

$$SI = \frac{(NDVI + LAI + FVC)}{3} \quad (2)$$

3.2.3.Response Indicator (RI)

Response indicators demonstrate how an ecosystem responds to changes in its overall health, including those caused by both human activities and natural processes within the ecosystem itself [38]. The response indicators typically indicate high-pressure situations, suggesting a severe ecological problem and numerous ecosystem changes. Therefore, high

responses were indicative of severe ecological disturbance or environmental change. Conversely, low reaction indicators indicate low state indicators, which suggest highly stable conditions or good environmental conditions and an established environment with minimal to no change resulting from reduced natural and human demand. It can be plainly stated that low response indices signify sustainable development and a regulated ecology. RI can be calculated from Eq. (3) [7].

$$RI = PI - SI \quad (3)$$

3.3. Calculation of Ecological Index (EI)

The ecological index (EI) contributes more to the ecological quality in the actual evaluation

$$EI = w(environment) + w(climate) + w(soil\ moisture) + w(greenness) + w(LCLU) + w(artificial\ features\ \&\ energy) + w(water\ content) + w(landscape) \quad (5)$$

where the Environmental parameter refers to the global environmental monitoring index (GEMI); Climate parameter: Soil moisture: soil adjusted vegetation index (SAVI) and normalized difference moisture index (NDMI); Greenness: normalized difference vegetation index (NDVI), leaf area index (LAI), and fractional vegetation cover (FVC); Land use/land cover: LULC change; Artificial features and energy: Road network and Railway network; Water content: normalized difference water index (NDWI); and Landscape: digital elevation model (DEM).

4. RESULTS AND DISCUSSION

The results of this study present a comprehensive examination of the Eco-environmental Quality (EEQ) assessment using the pressure-state-response (PSR) approach, along with an analysis of changes and a comparison of the EI between the winter and summer seasons in the study area in 2023. The precise outcomes are as follows:

4.1. Indicators Characteristic

4.1.1. Elevation

The DEM map shows the topographic phenomena of the region as it varies from (192 m) to (632 m), as shown in Fig. 12. The highest altitude is represented in the north of the study area, and it decreases as heading from north to south. The northeast, where Khasa is located, has the highest altitude, ranging from 481 m to 632 m. The southwest of the study area, where Taza is located, represents the lowest elevation, ranging from 192 m to 272 m. Generally, human socioeconomic activities and impacts decrease at high altitudes. Therefore, the environmental

conditions are much healthier than those at low altitudes, where human activities are increased.

$$EI = \sum_{i=1}^n W * C \quad (4)$$

Using all the ecological response parameters, the ecological indicator was calculated in this paper from Eq. (5).

conditions are much healthier than those at low altitudes, where human activities are increased.

4.1.2. Rail and Road Network

The road network in the center of Kirkuk City is denser in the middle than in the southwest. The railway network passes through the study area from the west to the north. The road and railway networks provide essential and consistent transportation services and regular transportation facilities for citizens. Thus, the road and railway network has a direct and proportional relationship with the population of a region, i.e., places with intensive road and railway networks have a higher human socioeconomic activity, resulting in less healthy environmental conditions, as shown in Fig. 9.

4.1.3. Land Use/Cover

Land use and land cover maps are essential for aiding knowledge of environmental modeling and water management. The land use/cover classes are directly affected by the region's weather conditions. Due to the predominantly rainy weather conditions in winter and the generally hot weather conditions in summer, the wetlands in the study area are more abundant in winter than in summer. The weather does not influence the urban class. Urban style is influenced by the socioeconomic activities of humans. However, Fig. 10 shows that the direction of urban development is heading from northeast to southwest of the study area. The overall accuracy, i.e., 98.57%, with a Kappa Coefficient of 97.91% in the classification of winter, is shown in Table 2. While the overall accuracy in summer was 96.43% with a Kappa Coefficient of 94.37%, as shown in Table 2.

Table 2 Land Cover/Use Details.

Classes	Winter		Summer	
	User Accuracy	Producer Accuracy	User accuracy	Producer Accuracy
Urban	97.44%	97.44%	88.10%	100.00%
Vegetation	100.00%	97.73%	100.00%	85.19%
Barren Soil	98.11%	100.00%	100.00%	98.59%
Water	100.00%	100.00%	100.00%	100.00%
Agriculture	95.03%	96.37%	91.28%	93.01%

4.2. General Assessment of PSR

4.2.1. Pressure Indicator

PI was derived from 9 indicators, assigning equal weights to each of them. The PI map shows high pressure in developed areas. Usually, developed areas are characterized by high socioeconomic human activities. Therefore, the center of the study area and the surrounding villages show an increase in PI. Extreme pressure is concentrated in the center of Kirkuk City, and it tends to be more in summer than in winter, as shown in Fig. 14. Due to human activities, which increase in summer more than in winter, the pressure was reduced at the margins of the region. Villages around Kirkuk City experienced moderate pressure because socioeconomic activities are relatively less intense than those inside the town, according to the Barren region station, which is known to be less populated in villages. The study area comprises many barren and green areas, which exhibit low pressure due to the small population in these areas. It is important to note that PI increases as the population in an area increases and vice versa.

4.2.2. State Indicator

The SI is mainly calculated from FVC, NDVI, and LAI. Due to Kirkuk City's hot summers and humid winters, the entire vegetation was in good to exceptional condition throughout the summer, with NDVI values over (0.4). The southwest of the study area is characterized by high vegetation; therefore, NDVI values are relatively higher in the south direction. Since both FVC and LAI are markers of healthy vegetation, they likewise displayed the same NDVI pattern. As can be seen by comparing the three vegetation indices, hot weather, high socioeconomic activity, and more significant human pressure all contributed to the ongoing deterioration of the vegetation, as shown in Fig. 17. The final SI map, which is shown in Fig. 15, displays the cumulative impact of all vegetation indicators. Due to market pressure to maintain output in line with food demand, the SI map revealed high levels of human pressure in both urban areas and agricultural land. SI is generally high in both seasons. However, it tends to be low in the southern part of the study area, where Taza is located, during the summer, and it is lower in winter.

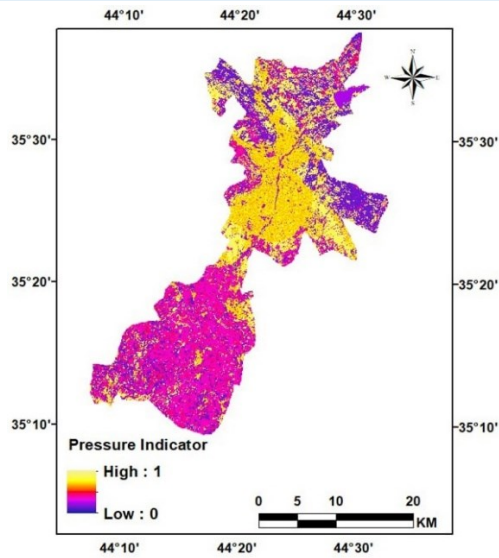
4.2.3. Response indicator (RI)

Under intense human pressure, weaker, less healthy, and more unstable ecological conditions are represented by higher response indicators, and vice versa. Increased RI values indicate increased natural/human pressure and socioeconomic activities, such as industrial expansion, farming, and urban growth, which can cause ecological disturbance. Low RI values indicate minimal human activity in ecosystems, such as those found in green lands and water bodies, as well as those located far from urban

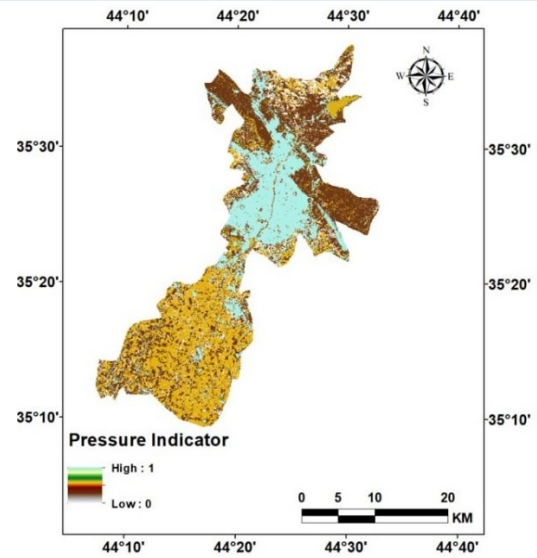
centers. Based on Fig. 16, the ecological state is continuously improving, as indicated by the RI maps. The study indicates that the area's south has superior ecological characteristics compared to its core region. It indicates that RI indices for the agriculture and cultivation sectors were lower than those for socioeconomic activity sites. However, the RI maps show that the ecological condition was better in winter than in summer, as human activity decreases, which in turn affects the RI value. One crucial factor in determining ecological change is the response indicator, which is part of the PSR framework created using remote sensing (RS) and GIS indicators. In addition to providing information on ecological conditions, it can be used by governmental and non-governmental organizations (NGOs) to guide policy decisions and support sustainable development. Response indicators indirectly reveal an area's growth or decline on the social or economic front, aiding in determining the overall evolution and changes in the area.

4.3. Ecological Index (EI)

Higher EI values indicate an ecological environment that is stable and healthy, and the reverse is true. Figure 17 shows a moderate to high EI value over the study area in both seasons. However, the center of Kirkuk City in summer has a lower EI value than in winter. The northeast and east of the study region were slightly better than the other parts, as they showed the highest values, distributed around Khasa and near Sulaymaniyah City to the east. Human activity increases in the central part of the study area, especially in summer. As a result, the center of Kirkuk City showed the lowest values, distributed over a considerably greater distance in summer than in winter. The south and the southwest of the study area, where Taza is located, showed a moderate EI value in both seasons. However, these values tend to be higher in winter than in summer, especially in some areas located to the south, as shown in Fig. 17. In other words, the regions near water bodies had outstanding EI conditions, according to the spatial distribution of EI maps, whereas the area next to it had excellent to moderate EI conditions. There were some industrial and residential areas with fair to bad ecological conditions. The north of the research area exhibited good to excellent ecological conditions, whereas the south exhibited good to fair ecology. Table 3 shows evaluations and their corresponding areas, as determined from Fig. 17. Unlike the Taza district, the center portion of the research region and Kirkuk City have fair to poor ecological conditions, indicating a dire need for an urgent intervention by an accountable and responsive ethical committee to address this serious issue.

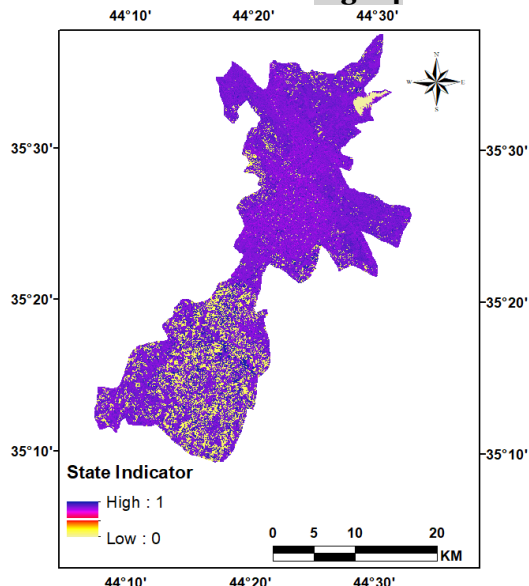


(a) PI for Winter Season.

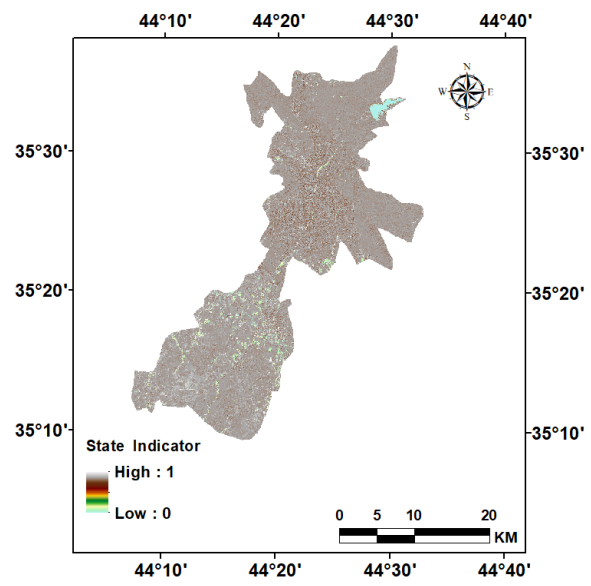


(b) PI for Summer Season.

Fig. 14 PI for Winter and Summer Seasons.

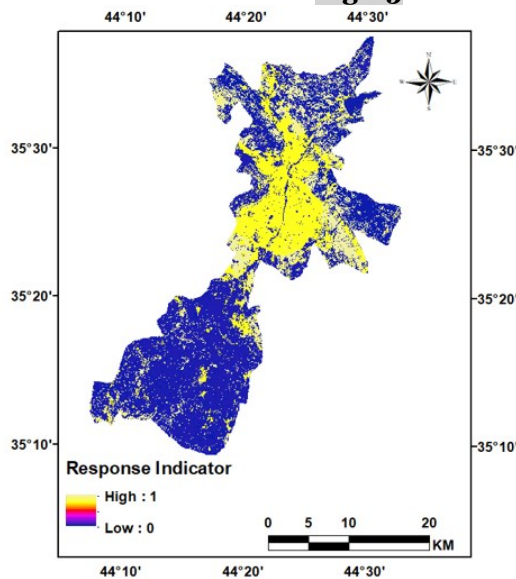


(a) SI for Winter Season.

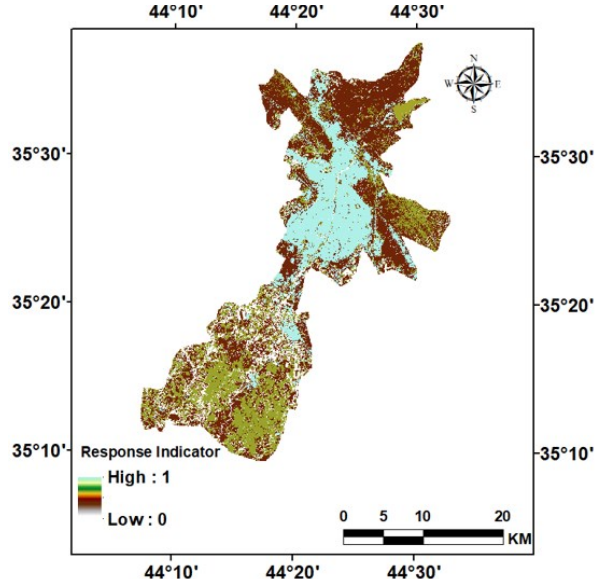


(b) SI for Summer Season.

Fig. 15 SI for Winter and Summer Seasons.



(a) RI for Winter Season.

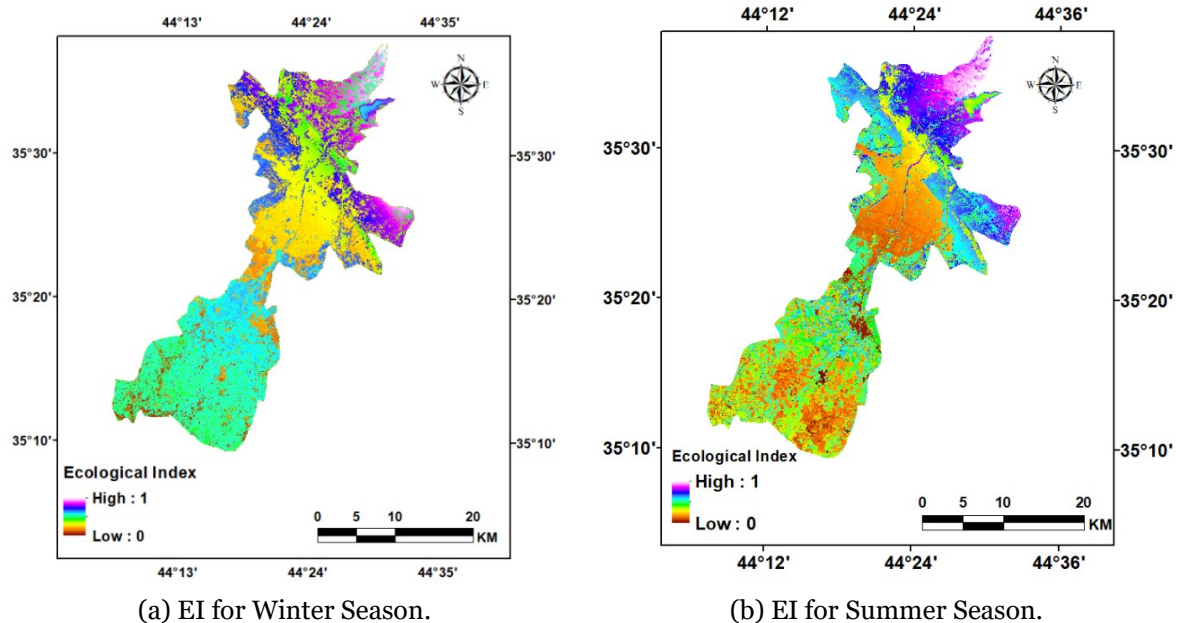


(b) RI for Summer Season.

Fig. 16 RI for Winter and Summer Seasons.

Table 3 Evaluations and their Corresponding Areas.

Evaluation	Winter (km ²)	Summer (km ²)
Extreme excellent – excellent	229.3	54.59
Excellent – good	142.5	187.91
Good – fair	165.93	244.69
Fair – poor	97.36	110.8
Poor – bad	44.65	81.75



4.4. General assessment of EEQ

This paper determines the ecological index to support the EEQ in Kirkuk City, Iraq. Due to the increased number of input indicators, EI is considered the most accurate index for evaluating environmental conditions. GIS and remote sensing technologies are considered the most common tools for monitoring EEQ in any region due to their ability to extract various factors related to land, water, and atmosphere, as well as their features. These tools provide access to previously forbidden and inaccessible areas, offering accurate, real-time information. Thus, this research, which aims for eco-environmentally sustainable development, is conducted in Kirkuk City, Iraq, using time-series remote sensing satellite data represented by Sentinel satellite images. Because this work was conducted under the PSR framework, which allows for the rapid and analytical assessment of eco-environmental quality (EEQ), 12 indicators associated with environmental issues were identified. Additionally, a pressure indicator was constructed to detect actual human and socioeconomic pressure, a state indicator to assess the pressure, and response indicators. Land use/cover change, human and natural pressure, the overall environment's condition, and the ecosystem's health were all considered when assessing the EEQ. The surrounding environment has been disturbed mostly by this intense land exploration and frequent human

impact. Human-socioeconomic activities must, therefore, be examined in the research of EEQ. SI reduced the pressure; hence, the state indicator was crucial in the EEQ analysis. As a result, the study area's green lands are essential for preventing environmental deterioration and creating stable ecological conditions. To preserve these green lands, more forests, mangroves, and wetland areas must be created throughout this decade. Any change in an ecosystem under various forms of pressure can be easily identified using response indicators under the PSR framework. Thus, an efficient method for mapping, tracking, and managing ecological issues at regional and global levels is devised in this research project, utilizing Remote sensing (RS) /GIS. The primary focus of this EEQ analysis was on the vegetative ecosystem as a means of lowering the pressure indicator and safeguarding ecology. The maximum number of metrics pertinent to topographic characteristics, complex climates, and natural conditions were calculated. It was noticed that the vegetative ecosystem had improved over the ecological monitoring period. In the vicinity of Kirkuk City and the central region of the study area, where land exploration was comparatively high due to particular human - socioeconomic socioeconomic activities, including farming and urban development. Human pressure has increased on the health of the surrounding vegetation ecosystems and the surrounding

natural environment. As a result, these regions exhibited high levels of human pressure, poor ecological conditions, and a greater need for attention and ongoing ecological monitoring to protect them. The EEQ assessment identifies specific locations that have been protected by the government to preserve ecological integrity and minimize the impact of human pressure compared to unprotected regions. As a result, specific regulations for a stable and healthy environment must be created and appropriately implemented in the necessary areas. Since all of the parameters, indicators, and determinants in this research effort have broad applications, their development is crucial for NGOs, government policymakers, and those involved in sustainable development.

5.CONCLUSIONS

Using GIS and remote sensing data, this paper examines the eco-environmental condition by calculating the key ecological indicators under the PSR framework to assess the EEQ. The EI showed a sensible condition of the study area based on various indicators that measure different impacts on the environmental system. The paper identifies:

- Whereas dryness and heat/temperature indicators negatively affect a healthy environment, the indicators that represented greenness and wetness demonstrated a positive response.
- The EEQ improvement is based on all the positive values reflected from the natural responses.
- Ecological health is significantly influenced by human activities, including the social and economic activities that negatively impact the system.

ACKNOWLEDGEMENTS

The authors express their heartfelt appreciation to all those who offered assistance and made contributions that greatly aided the successful culmination of this research work. This work is based on a postgraduate thesis that was submitted to the Surveying Engineering Techniques Department at the Engineering College of Kirkuk, Northern Technical University. The thesis was submitted under University Order 4266 on September 4, 2023.

REFERENCES

- [1] Wang X, Cao Y, Zhong X, Gao P. A New Method of Regional Eco-Environmental Quality Assessment and Its Application. *Journal of Environmental Quality* 2012; **41**(5):1393-1401.
- [2] Ma H, Shi L. Assessment of Eco-Environmental Quality of Western Taiwan Straits Economic Zone. *Environmental Monitoring and Assessment* 2016; **188**(5): 311.
- [3] Duda AM, El-Ashry MT. Addressing the Global Water and Environment Crises Through Integrated Approaches to the Management of Land, Water and Ecological Resources. *Water International* 2000; **25**(1):115-126.
- [4] Li J, Pei Y, Zhao S, Xiao R, Sang X, Zhang C. A Review of Remote Sensing for Environmental Monitoring in China. *Remote Sensing* 2020; **12**(7):1-25.
- [5] Das S, Pradhan B, Shit PK, Alamri AM. Assessment of Wetland Ecosystem Health Using the Pressure-State-Response (PSR) Model: A Case Study of Mursidabad District of West Bengal (India). *Sustainability* 2020; **12**(15): 5932.
- [6] Xiong J, Li W, Zhang H, Cheng W, Ye C, Zhao Y. Selected Environmental Assessment Model and Spatial Analysis Method to Explain Correlations in Environmental and Socio-Economic Data with Possible Application for Explaining the State of the Ecosystem. *Sustainability* 2019; **11**(17): 4781.
- [7] Boori MS, Choudhary K, Paringer R, Kupriyanov A. Eco-Environmental Quality Assessment Based on Pressure – State - Response Framework by Remote Sensing and GIS. *Remote Sensing Applications: Society and Environment* 2021; **23**: 100530.
- [8] Sun R. Effects of Land-Use Change on Eco-Environmental Quality in Hainan Island, China. *Ecological Indicators* 2020; **109**(4):105777.
- [9] Shareef MA, Hassan ND, Hasan SF, Khenchaf A. Integration of Sentinel-1A and Sentinel-2B Data for Land Use and Land Cover Mapping of the Kirkuk Governorate, Iraq. *International Journal of Geoinformatics* 2020; **16**(3):87-96.
- [10] Yue H, Liu Y, Li Y, Lu Y. Eco-Environmental Quality Assessment in China's 35 Major Cities Based on Remote Sensing Ecological Index. *IEEE Access* 2019; **7**:51295-51311.
- [11] Burton P, Woolcock G, Matthews T, Procter M. Green Star Communities Information Papers - Draft Final Report. *Green Star* 2010; (October) Urban Research Program Griffith University.
- [12] Pacione M. Urban Environmental Quality and Human Wellbeing - A Social Geographical Perspective. *Landscape and Urban Planning* 2003; **65**(1-2):19-30.

- [13] Salahalden VF, Shareef MA, Nuaimy QAA. **Red Clay Soil Physical and Chemical Properties Distribution Using Remote Sensing and GIS Techniques in Kirkuk City, Iraq.** *Iraqi Geological Journal* 2024; 57(1):194-220.
- [14] Pinty AB, Verstraete MM. **GEMI: A Non-Linear Index to Monitor Global Vegetation from Satellites.** *Vegetatio* 2011; 101(1):15-20.
- [15] Kareem HH, Omran ZA, Attaee MH. **Detection the Impact of Chlorophyll Index and Global Environmental Monitoring Index on Water Separation in Swansea in Wales, United Kingdom Through Analysing the Spectral Wavelengths of Landsat 8-OLI.** *Ecological Engineering and Environmental Technology* 2023; 24(9):259-270.
- [16] Chu D. **Fractional Vegetation Cover, or FVC, is a Crucial Metric in the Study of Soil Erosion, Climate Change, and Ecosystem Balance.** 2019.
- [17] Carlson TN, Ripley DA. **On the Relation Between NDVI, Fractional Vegetation Cover, and Leaf Area Index.** *Remote Sensing of Environment* 1997; 62(3):241-252.
- [18] Fang H, Baret F, Plummer S, Schaepman-Strub G. **An Overview of Global Leaf Area Index (LAI): Methods, Products, Validation, and Applications.** *Reviews of Geophysics* 2019; 57(3):739-799.
- [19] Zheng G, Moskal LM. **Retrieving Leaf Area Index (LAI) Using Remote Sensing: Theories, Methods and Sensors.** *Sensors* 2009; 9(4):2719-2745.
- [20] Rahman S, Mesev V. **Change Vector Analysis, Tasseled Cap, and NDVI-NDMI for Measuring Land Use/Cover Changes Caused by a Sudden Short-Term Severe Drought: 2011 Texas Event.** *Remote Sensing* 2019; 11(19): 2217.
- [21] Shareef MA, Hasan SF. **Characterization and Estimation of Dates Palm Trees in an Urban Area Using GIS-Based Least-Squares Model and Minimum Noise Fraction Images.** *Journal of Ecological Engineering* 2020; 21(6):78-85.
- [22] Strashok O, Ziemiańska M, Strashok V. **Evaluation and Correlation of Sentinel-2 NDVI and NDMI in Kyiv (2017-2021).** *Journal of Ecological Engineering* 2022; 23(9):212-218.
- [23] McFeeters SK. **NDWI by McFEETERS.** *Remote Sensing of Environment* 1996; 25(3):687-711.
- [24] Wang X, Yan Y, Cao Y. **Impact of Historic Grazing on Steppe Soils on the Northern Tibetan Plateau.** *Plant and Soil* 2012; 354(1-2):173-183.
- [25] Neri AC, Dupin P, Sánchez LE. **A Pressure-State-Response Approach to Cumulative Impact Assessment.** *Journal of Cleaner Production* 2016; 126:288-298.
- [26] Hasan SF, Shareef MA, Hassan ND. **Speckle Filtering Impact on Land Use/Land Cover Classification Area Using the Combination of Sentinel-1A and Sentinel-2B (A Case Study of Kirkuk City, Iraq).** *Arabian Journal of Geosciences* 2021; 14(4):276.
- [27] Shareef MA, Ameen MH, Ajaj QM. **Change Detection and GIS-Based Fuzzy AHP to Evaluate the Degradation and Reclamation Land of Tikrit City, Iraq.** *Geodesy and Cartography* 2020; 46(4):194-203.
- [28] Comber A, Wulder M. **Considering Spatiotemporal Processes in Big Data Analysis: Insights from Remote Sensing of Land Cover and Land Use.** *Transactions in GIS* 2019; 23(5):879-891.
- [29] Rhyma PP, Norizah K, Hamdan O, Faridah-Hanum I, Zulfa AW. **Integration of Normalised Different Vegetation Index and Soil-Adjusted Vegetation Index for Mangrove Vegetation Delineation.** *Remote Sensing Applications: Society and Environment* 2020; 17:100280.
- [30] Huete AR. **A Soil-Adjusted Vegetation Index (SAVI).** *Remote Sensing of Environment* 1988; 25(3):295-309.
- [31] Zhou Q. **Digital Elevation Model and Digital Surface Model.** *International Encyclopedia of Geography* 2017; (March):1-17.
- [32] Vaze J, Teng J, Spencer G. **Impact of DEM Accuracy and Resolution on Topographic Indices.** *Environmental Modelling and Software* 2010; 25(10):1086-1098.
- [33] Neteler M. **Estimating Daily Land Surface Temperatures in Mountainous Environments by Reconstructed MODIS LST Data.** *Remote Sensing* 2010; 2(1):333-351.
- [34] Hulley GC, Ghent D, Götsche FM, Guillevic PC, Mildrexler DJ, Coll C. **Land Surface Temperature.** In *Taking the Temperature of the Earth* (pp. 57-127). Elsevier ;2019.
- [35] Ren W, Zhang X, Peng H. **Evaluation of Temporal and Spatial Changes in Ecological Environmental Quality on Jiangnan Plain From 1990 to**

2021. *Frontiers in Environmental Science* 2022; **10**(May):1-14.
- [36] Wolfslehner B, Vacik H. **Evaluating Sustainable Forest Management Strategies with the Analytic Network Process in a Pressure-State-Response Framework.** *Journal of Environmental Management* 2008; **88**(1):1-10.
- [37] Ji J, Chen J. **Urban Flood Resilience Assessment Using RAGA-PP and KL-TOPSIS Model Based on PSR Framework: A Case Study of Jiangsu Province, China.** *Water Science and Technology* 2022; **86**(12):3264-3280.
- [38] Liu D, Hao S. **Ecosystem Health Assessment at County-Scale Using the Pressure-State-Response Framework on the Loess Plateau, China.** *International Journal of Environmental Research and Public Health* 2017; **14**(1): 2.
- [39] Huang HF, Kuo J, Lo SL. **Review of PSR Framework and Development of a DPSIR Model to Assess Greenhouse Effect in Taiwan.** *Environmental Monitoring and Assessment* 2011; **177**(1-4):623-635.
- [40] **Evaluation of the Spatiotemporal Variations in the Eco-Environmental Quality in China Based on the Remote Sensing Ecological Index.** *Remote Sensing* 2020; **12**(15): 2462.